学位論文

Effects of the physical properties of facial soft tissues on facial displacement during smiling in patients with repaired unilateral cleft lip with or without palate

2018 年 3 月

大阪大学大学院歯学研究科　口腔科学専攻

(顎顔面口腔矯正学教室)

Donghoon Lee

指導教員：山城　隆　教授(顎顔面口腔矯正学教室)

INTRODUCTION

Patients with unilateral cleft lip with or without palate (UCL±P) receive a primary lip surgery usually at 2-4 months after their birth. Lip surgeries leave scar tissue at the lip region and dysmorphology remains even after surgery, which may elevate the risk of psychological distress and morbidity (Turner et al., 1998; Millar, 2013). Distorted facial motions during facial expressions (e.g., smiling) in the upper lip areas have been reported in patients with CL±P (Trotman et al., 2007; Barlow et al., 2012). Facial expressions play an important role as a means of nonverbal communication in the transmission of emotions and thoughts in social life; thus, facial expressions exert a strong influence on individuals in obtaining socially acceptable self-image. From a sociopsychological perspective, establishing an acceptable facial appearance including motions in patients with UCL±P is one of the crucial treatment goals in surgical/orthodontic clinics (Ackerman et al., 1998; Trotman et al., 2007).

There have been several assumptions to explain the causative factors of distorted facial motion in patients with UCL±P, but thus far, no report had clarified these factors (Essick et al., 2007; Barlow et al., 2012). It has been reported that increased elastic modulus of scar tissue of body skin is related to less extensibility (Dunn et al., 1985; Corr et al., 2009). Thus, in patients with UCL±P, it is hypothesized that the physical property of soft tissue around scarring in the naso-labial region would restrict facial functional movement during facial expressions.

Thus far, clinical assessment of facial appearance basically dependent on two-dimensional (2D) photography, which has limitations that they depict three-dimensional (3D) subjects in 2D photography (Honrado et al., 2006). Several

researches showed greater accuracy in 3D photography when compared with direct anthropometry and 2D photography (Lane and Harrel, 2008; Lübbers et al., 2010; Claes et al., 2012).

The objective of this research is following; 1) to determine the 3D facial displacement during smiling in patients with a repaired UCL±P differs in comparison with that of healthy adults (Experiment 1), 2) to calculate the random measurement error in the measurement of physical properties of facial soft tissue in healthy adults (Experiment 2), 3) to investigate whether physical properties of facial soft tissue are different between patients with a repaired UCL±P and healthy adults (Experiment 3), 4) to clarify the relationship between physical properties of facial soft tissues on 3D facial displacement during smiling in patients with repaired UCL±P (Experiment 4).

MATERIAL AND METHODS

The study protocol was approved by the Ethical Committee of the Graduate School of Dentistry, Osaka University (IRB No. H20-E19-2). An institutional review board-approved written informed consent form was distributed to and signed by all participants prior to involvement in the study.

Experiment 1 (Displacement of facial soft tissue during smiling)

Participants

Japanese patients with a repaired UCL±P (Cleft group; n = 41, mean age = 21.46 ± 4.27 years, 21 males and 20 females) and healthy adults featuring a straight type facial profile with a normal occlusion (Control group; n = 41, mean age = 25.78 ±

3.35 years, 21 males and 20 females) were enrolled in the present study. The inclusion criteria of the Cleft group were as follows: age range 15–37 years, no facial paralysis, no noticeable scars or skin diseases of the neck or dentofacial regions (or history thereof), no history of any psychiatric disorder, no subjectively or objectively discernible jaw dysfunction, a BMI ranging from 18.50 to 24.99 (World Health Organization, 2013), no maxilla-facial plastic surgeries in the past 6 months. The inclusion criteria of the Control group were as follows: age range 18–35 years, no congenital facial deformities including cleft lip or palate, no facial paralysis, no noticeable scars or skin diseases of the neck or dentofacial regions (or history thereof), no history of any psychiatric disorder, no subjectively or objectively discernible jaw dysfunction, a BMI ranging from 18.50 to 24.99 (World Health Organization, 2013), overbite ranging from 1.0–5.0 mm, overjet ranging from 0.0–7.0 mm, and a straight-type facial profile.

Data acquisition

The subjects were asked to sit on a fixed chair with a natural head position without head support. They were then asked to perform tasks as described in Table 1 (i.e., at rest and at the peak of the maximum smile) following our previous study (Tanikawa and Takada, 2017). The subjects were instructed vocally for each task and asked to maintain the expressions for about 2 seconds. After several rehearsals, each expression was recorded once with a three-dimensional image capturing device (3dMDcranial System, 3dMD, Atlanta, GA, USA) (Fig. 1). Each type of expression was recorded with a resting interval of about 20 seconds between the expressions. The experimenter (D. L.) operated the system from a position out of the subject's view. The room temperature was set at 25°C.

Each 3D facial image was displayed on a computer monitor. The positions of seven single and five paired landmarks were identified by visual inspection of the image

and digitized using a computer mouse cursor and commercial software (3D-Rugle Version 5.5, Medic Engineering Co., Kyoto, Japan). The process was repeated twice for each image, and the landmark coordinates from the two digitizations produced were averaged to yield the final landmark coordinates.

Coordinate system

A coordinate system of the 3D images recorded at rest was established based on our previous study (Fig. 2) (Tanikawa et al., 2007; Tanikawa et al., 2010). The images recorded at the peak of the maximum smile were then standardized using the common coordinate system on the basis of the 19 square regions (Fig. 3; size, 4.0 × 4.0 mm; each square included 81 points) located on the forehead and the nasal bridge. These areas were assumed to be the immobilized regions during smiling. For the standardization process, we employed the Iterative Closest Point algorithm (For more details of the calculation, please see Appendix 1). The mean anteroposterior distance between the two facial postures for the 19 square regions was 0.26 mm and was considered to be sufficiently small for subsequent calculation.

To standardize the differences in facial size, the images were normalized on the distance between the right and left *exocanthions*. Mirror images of the patients with right cleft lips were mathematically created to produce images for patients with left cleft lips.

Analysis

(1) 3D averaged faces for each facial expression

Wire mesh fitting and averaged faces. For each participant, a wire mesh fitting based on the assignment of landmarks to each 3D facial image was performed using the software (Face-Rugle Version 1.01, Medic Engineering Co., Kyoto, Japan). This method generated 6,017 points on the wire mesh (i.e., the nodes of the fitted mesh) for each

facial expression (Fig. 4). The arithmetic mean of the coordinate values and the color values of each corresponding point on the wire mesh were computed and used to generate the 3D averaged facial images for each subject group and for each facial expression (Fig. 5).

(2) Examination of the displacement from the rest to the peak of the maximum smile

To determine displacement in the soft tissue surface morphology from rest to the peak of the maximum smile, displacement of each point on the facial surface in the X, Y, and Z axis between the two facial postures was calculated. A two-sample *t*-test was performed to compare the displacement of two subject groups in each axis (Fig. 6). To visualize difference of displacement between two subject groups, the results were represented as a color map showing the p-values for the aforementioned comparison between two subject groups (hereafter, significance probability map) and a color map representing the differences between the displacements during smiling between two subject groups (hereafter, distance map) (Kono et al., 2017; Tanikawa and Takada, 2017). The statistically significant level was set at $P \leq 0.05$.

Craniofacial characteristics

To obtain baseline information of craniofacial characteristics of the patients in the Cleft group, cephalometric radiographs of the patients which were taken within 6 months of the time point when 3D facial images were taken were obtained, digitized, traced, and analyzed by one experimenter (D.L.) using a commercial software (Dolphin Imaging 11.0, Dolphin Imaging & Management Solutions, Chatsworth, Calif) with regard to the 13 cephalometric parameters (for the definition of the parameters, please see Appendix 2). Further, we also examined the differences in 3D facial surfaces between the Control group and the Cleft group in the Z-values by means of the significance

probability map and the distance map.

Experiment 2 (Intermediate precision in the measurement of viscoelasticity)

Participants

Eleven adult volunteers (six males and five females, age range 25 - 32 years) were randomly selected from the Control group for the evaluation of the minimal detectable change in the measurement.

Data acquisition

The elastic modulus (kN/m²) and viscosity coefficient (N·s/m²) of facial landmarks including the *cheek* (*Chk*), *crista philtri superior'* (*Cphs'*), *crista philtri inferior* (*Cphi*), and *cheilion* (*Ch*) on the left side were measured by using a viscoelasticity measuring instrument (Vesmeter-E100Hs, WaveCyber Corp., Saitama, Japan) (Fig. 7). The definition of *Cphi* and *Ch* was based on anthropometric investigations described by Mulliken et al. (2001). *Cphs'* was defined as the point on the philtral crest where about 12mm below of the *crista philtri superior* which was defined by Mulliken et al. (2001) because of the limitation of measurement from the size of the probe of viscoelasticity measuring instrument. *Chk* was defined as the most prominent point of cheek. The room temperature was set at 25°C. Every measurement was conducted three times at each landmark and an average value of three measurements was employed for statistical analysis. These measurements were repeated on two separate occasions, Session 1 and Session 2, with an interval of one week between sessions.

Statistical analysis

The minimal detectable change at the 95% confidence level (MDC_{95}) was calculated for each landmark based on Bland - Altman analysis (Bland and Altman, 1986) using the following equations:

$$MDC_{95} = SEM \times 1.96\, x\sqrt{2} \quad (1)$$

In equation 1, the standard error of measurements (SEM) was calculated using the following equation:

$$SEM = \frac{SD_d}{\sqrt{2}} \quad (2)$$

The MDC_{95} were calculated for the following regions: *Chk*, *Cphs'*, *Cphi,* and *Ch*.

Experiment 3 (Comparison of viscoelasticity between the Cleft group and the Control group)

Data acquisition

The Control and Cleft groups of Experiment 1 were enrolled in the present experiment. The elastic modulus (N/m^2), and viscosity coefficient ($N \cdot s/m^2$) of the facial soft tissues at four landmarks (i.e., *Chk*, *Cphs'*, *Cphi*, and *Ch;* defined in the Experiment 2*)* were measured at left and right sides in both groups using a viscoelasticity measuring instrument following the method described in the Experiment 2.

Statistical analysis

A two-sample t-test was used to examine whether there were any significant differences in elastic modulus and viscosity coefficient between the Cleft group and the Control group. Normal distribution of the data was statistically confirmed by using the

Kolmogorov-Smirnov test. When mean differences between groups showed the values more than the MDC_{95} defined in the Experiment 3 and P-values less than 0.05 were observed, we defined there was a statistically significant difference.

Experiment 4 (Relationship between viscoelasticity and displacement of facial soft tissue)

Data analysis

Three-dimensional facial surfaces at rest and at the peak of the smiling in the Experiment 1; and the elastic modulus and viscosity coefficient of the facial soft tissues at four landmarks in the Experiment 3 for the Cleft group were used in the present experiment.

K-means clustering procedure

To detect the coherent patterns in the Cleft group in details, sixteen parameters of two physical properties, i.e., elastic modulus and viscosity coefficient, at the four landmarks (*Chk, Cphs', Cphi*, and *Ch*) on both sides were entered into the following procedure. First, the principal component analysis (PCA) was employed to reduce the number of parameter dimensions. In the present study, ten parameters in the component space that accounted for 95% of the variance were determined by the PCA. Second, reduced dimensional data were subdivided into k-clustering classifiers (MacQueen, 1967). Details of the calculation are as follows: The first step was to define k centroids, one for each cluster that was randomly selected. The next step was to take each data and associate the data to the nearest centroid. Then, k new centroids were re-calculated and data was associated with the nearest new centroid. The process was

iterated, where k centroids changed their location until no more changes were made (Gonzalez et al., 2011). In short, in this study, we subdivided the 41 participants of the Cleft group into three clusters (Codes) based on 16 parameters representing their viscoelastic characteristics of the facial soft tissue.

Differences among Codes and the corresponding dentofacial characteristics in each Code

Firstly, to examine the characteristics of physical properties in each code, A significant difference of physical properties of facial landmarks among Codes was examined using a one-way ANOVA, Tukey post-hoc test and MDC_{95} ($P < 0.05$). A significant difference of physical properties between the cleft side and non-cleft side in each Code was also evaluated using a paired t-test and MDC_{95} ($P < 0.05$).

Further, to examine the corresponding dentofacial characteristics in each Code, a significant difference among Codes was examined using one-way ANOVA ($P < 0.05$).

Lastly, to examine the corresponding tomographic characteristics of the 3D facial displacements between at rest and at the peak of the smile in each Code, the areas that showed significant facial displacement during smiling were examined in each Code using a paired t-test ($P < 0.05$). To visualize the significant displacement during smiling, a significance probability map was generated ($P < 0.05$).

RESULTS

Experiment 1

Craniofacial characteristics of patients in the Cleft group were shown in Appendices 2 and 3. In short, the cephalometric analysis revealed that there were no

significant differences in ANB angles between the previously reported controls and the present Cleft group, indicating our samples were considered as the normal skeletal relationships. Figure 8 provides the results of the statistical comparisons between the subject groups for each area.

Difference of displacement during smiling between the Cleft group and the Control group

Cheek. In the horizontal direction (X–axis), the Cleft group showed less lateral displacement than the Control group on the non-cleft side by approximately 2 mm ($P < 0.001$) (Table 2). There was no significant difference of displacement between two groups on the cleft side (Table 3). In the vertical direction (Y-axis), the Cleft group showed less upward displacement than the Control group on both sides by approximately 2 mm and the difference between two groups was greater on the non-cleft side ($P < 0.0001$) than the cleft side ($P < 0.01$). In the anteroposterior direction (Z-axis), however, no significant difference of displacement was found between two subject groups.

Nasal dorsum. In the horizontal direction, there was no significant difference of displacement between two groups. In the vertical direction, the Cleft group showed less upward displacement than the Control group on the non-cleft side by approximately 1mm ($P < 0.05$). In the anteroposterior direction, the Cleft group showed less backward displacement than the Control group on the non-cleft side by approximately 1.5 mm ($P < 0.05$).

Alar. In the horizontal direction, the Cleft group showed less lateral displacement than the Control group on the non-cleft side by approximately 2 mm ($P < 0.01$). In the vertical direction, the Cleft group showed less upward displacement than the Control group on the non-cleft side by approximately 2 mm ($P < 0.01$). In the anteroposterior direction, the

Cleft group showed less backward displacement than the Control group on both sides by approximately 1.5 mm and the difference was greater on the cleft side ($P < 0.01$) than the non-cleft side ($P < 0.05$).

Subalar. In the horizontal direction, the Cleft group showed greater lateral displacement than the Control group on the cleft side by approximately 1.5 mm ($P < 0.05$). In the vertical direction, no significant difference of upward displacement was found between two groups. In the anteroposterior direction, the Cleft group showed less backward displacement than the Control group on the cleft side by approximately 2 mm ($P < 0.05$).

Upper lip. In the horizontal direction, no significant difference of displacement was found between two groups. In the vertical direction, the Cleft group showed less upward displacement than the Control group on both sides by approximately 2mm ($P < 0.01$). In the anteroposterior direction, the Cleft group showed less backward displacement than the Control group on the cleft side by approximately 2 mm ($P < 0.0001$)

Lower lip. In the horizontal and anteroposterior directions, no significant difference of displacement between two groups was found. In the vertical direction, the Cleft group showed greater downward displacement than the Control group on both sides by approximately 3 mm ($P < 0.01$).

Labial commissure. In the horizontal direction, no significant difference of displacement between two groups was found. In the vertical direction, the Cleft group showed less upward displacement than the Control group on both sides by approximately 3 mm ($P < 0.01$). In the anteroposterior direction, the Cleft group showed less backward displacement than the Control group on both sides by approximately 2 mm on average and the difference was greater on the cleft side ($P < 0.01$) than the non-cleft side ($P < 0.05$).

Chin. In the horizontal, vertical, and anteroposterior directions, no significant difference of displacement between two groups was found.

Experiment 2

MDC_{95} of elastic modulus and viscosity coefficient at each landmark was calculated and results are shown in Table 4. Mean value of MDC_{95} in four landmarks was 39.40 kN/m^2 for elastic modulus and 127.31 N・s/m^2 for viscosity coefficient, respectively. The maximum value of MDC_{95} was 48.52 kN/m^2 for elastic modulus which was found at *Chk* and 168.06 N・s/m2 for viscosity coefficient which was found at *Cphi*. The minimum value of MDC_{95} was 20.73 kN/m^2 and 80.04 N・s/m^2, for elastic modulus and viscosity coefficient respectively, which was found both at *Ch*. In Experiments 3 and 4, the difference of viscoelasticity between two subjects of each landmark was judged as significant when it is above the MDC_{95} of each landmark.

Experiment 3

Normal distribution of physical properties in each group was clarified. The Cleft group showed significantly greater elastic modulus than the Control group at *Cphs'* on the cleft side, indicating the stiffer character of the scar than normal skin ($P < 0.05$) (Fig. 9). The standard deviation of elastic modulus was greater in the Cleft group than the Control group at all landmarks except *Cphi* on both sides. There was no significant difference of viscosity coefficient between two groups (Fig. 10). The standard deviation of viscosity coefficient was greater in the Cleft group than the Control group at all landmarks except at *Cphs'* on the non-cleft side.

Experiment 4

The Cleft group was successfully subcategorized into three subgroups (Codes

1, 2, and 3) based on physical properties of facial soft tissue. The characteristics of physical properties in each code and the corresponding facial displacements during smiling were as follows.

Characteristics of physical properties in each Code

Code 1 (n = 19) showed significantly less elastic modulus than Codes 2 and 3 at all the landmarks on both sides (Fig. 11). Code 3 (n = 7) showed significantly greater elastic modulus than Code 1 at all landmarks and Code 2 at *Cphi* on the non-cleft side. Code 3 showed significantly greater viscosity coefficient at the *Ch* and *Cphi* on both sides and at the *Chk* on the cleft side when compared to Code 1. Code 2 (n = 15) showed the intermediate character of viscoelasticity between Codes 1 and 3. Significantly greater elastic modulus was observed on the cleft side when compared to the non-cleft side at *Cphs'* in Codes 1 and 3 and its difference was greater in Code 3 than Code 1 ($P < 0.05$).

Comparison of dental and skeletal parameters among Codes

There was no significant difference of dental and skeletal parameters among Codes ($P > 0.05$) (Table 5).

Characteristics of facial displacement during smiling in each Code

Cheek. In the horizontal direction (X-axis), all Codes showed significant lateral displacement whereas Codes 1 and 2 showed lateral displacement by approximately 5.5mm with symmetrical appearance ($P < 0.0001$) (Fig. 12) (Table 6). Otherwise, Code 3 showed greater lateral displacement on the cleft side ($P < 0.0001$) than the non-cleft side ($P < 0.001$). In the vertical direction (Y-axis), Codes 1 and 2 showed significant upward displacement by approximately 3.5mm on both sides (Table 7). Code 3 showed

no significant upward displacement on both sides. In the anteroposterior direction (Z-axis), Code 1 showed significant forward displacement by approximately 3mm on both sides and greater displacement was observed on the non-cleft side ($P < 0.01$) than the cleft side ($P < 0.05$) (Table 8). Code 2 showed significant forward displacement by approximately 3.5mm on both sides with symmetrical appearance ($P < 0.05$). Code 3 showed significant forward displacement only on the cleft side by approximately 3.5mm ($P < 0.05$).

Nasal dorsum. There was no significant displacement both in horizontal and anteroposterior directions of all Codes. In the vertical direction, only Code 2 showed upward displacement by approximately 2.5mm on both sides ($P < 0.05$).

Alar. In the horizontal direction, all Codes showed significant lateral displacement by approximately 3mm ($P < 0.05$) on both sides. In the vertical direction, Codes 1 and 2 showed upward displacement by approximately 3mm on both sides ($P < 0.05$). Otherwise, there was no significant upward displacement in Code 3. In the anteroposterior direction, there was no significant displacement in all Codes.

Subalar. In the horizontal direction, Code 1 showed significant lateral displacement on both sides and greater displacement was observed on the cleft side ($P < 0.001$) than the non-cleft side ($P < 0.01$). Code 2 showed significant lateral displacement by approximately 2.5mm on both sides with symmetrical appearance. Code 3 showed significant lateral displacement by approximately 2mm only on the cleft side which is consistent with the result of Experiment 1 ($P < 0.01$). In the vertical direction, Code 1 showed significant upward displacement by approximately 3mm on both sides ($P < 0.05$). Code 2 showed significant upward displacement by approximately 4.5mm on both sides ($P < 0.01$). Otherwise, Code 3 showed no significant upward displacement. In the anteroposterior direction, Codes 1 and 2 showed significant backward displacement by approximately 4.5mm on both sides with symmetrical appearance ($P <$

0.01). Code 3 showed significant backward displacement by approximately 3mm only on the non-cleft side ($P < 0.05$).

Upper lip. In the horizontal direction, Code 1 showed significant lateral displacement by approximately 3.5mm on both sides ($P < 0.01$). Code 2 showed significant lateral displacement by approximately 3mm on both sides ($P < 0.01$). Code 3 showed significant lateral displacement by approximately 1.5mm on both sides ($P < 0.05$). In the vertical direction, Code 1 showed significant upward displacement by approximately 5.5 mm on both sides ($P < 0.01$). Code 2 showed significant upward displacement by approximately 6mm on both sides ($P < 0.001$). Otherwise, Code 3 showed no significant displacement on both sides. In the anteroposterior direction, Codes 1 and 2 showed significant backward displacement by approximately 8.5mm on both sides ($P < 0.0001$). Code 3 showed significant backward displacement by approximately 7.5mm on both sides ($P < 0.01$).

Lower lip. In the horizontal direction, Code 1 showed significant lateral displacement by approximately 3.5mm on both sides ($P < 0.0001$). Code 2 showed significant lateral displacement by approximately 3mm on both sides ($P< 0.001$). Code 3 showed significant lateral displacement by approximately 2.5mm on both sides ($P < 0.01$). In the vertical direction, Codes 1 and 3 showed no significant displacement on both sides. Otherwise, Code 2 showed significant downward displacement by approximately 3.5mm on both sides ($P < 0.05$). In the anteroposterior direction, Code 1 showed significant backward displacement by approximately 8.5mm on both sides ($P < 0.001$). Code 2 showed significant backward displacement by approximately 7.5mm on both sides ($P < 0.01$). Code 3 showed significant backward displacement on both sides and greater displacement was observed on the non-cleft side ($P < 0.01$) than the cleft side ($P < 0.05$).

Labial commissure. In the horizontal direction, Codes 1 and 2 showed significant

lateral displacement by approximately 7.5mm on both sides with symmetrical appearance ($P < 0.0001$). Otherwise, Code 3 showed significant lateral displacement on both sides and greater displacement was observed on the cleft side ($P < 0.0001$) than the non-cleft side ($P < 0.01$). In the vertical direction, Codes 1 and 2 showed significant upward displacement by approximately 7.5mm on both sides ($P < 0.0001$). Code 3 showed significant upward displacement by approximately 4.5mm on both sides ($P < 0.05$). In the anteroposterior direction, Codes 1 and 2 showed significant backward displacement by approximately 8.5mm on both sides with symmetrical appearance ($P < 0.0001$). Otherwise, Code 3 showed significant backward displacement on both sides and greater displacement was observed on the non-cleft side ($P < 0.0001$) than the cleft side ($P < 0.01$).

Chin. In the horizontal and anteroposterior directions, there was no significant displacement in the chin area of all Codes. In the vertical direction, only Code 2 showed downward displacement by approximately 3.5mm on both sides.

Overall, it was found that physical property of facial soft tissue affected facial displacement during smiling in the Cleft group.

DISCUSSION

To the best of our knowledge, this is the first attempt to evaluate the relationship between the physical property of the scar with surrounding soft tissue and facial displacement in patients with UCL±P. Our results regarding the displacement of facial soft tissue during smiling revealed that patients with UCL±P showed interrupted displacement of facial soft tissue during smiling in the Experiment 1. Further, in the

Experiment 2, we determined the minimal detectable change of physical property of facial soft tissue for each landmark, which was employed for the analysis in the Experiments 3 and 4 when examining the physical properties. In the Experiment 3, we found greater viscoelasticity of the scar and surrounding facial soft tissue in patients with UCL±P than in healthy adults. Finally, we clarified the relationship between viscoelasticity of the scar and surrounding facial soft tissue and displacement of facial soft tissue during smiling in patients with UCL±P in the Experiment 4. Details of the findings were discussed as follows.

Measuring device

We demonstrated the entire 3D facial surface analysis associated with smiling in patients with UCL±P, in an objective and site-specific manner. Thus far, there were several reports examining facial displacement in patients with CL±P. For example, Offerman et al. (1994) employed 2D photographs before and after smiling from the frontal view and reported greater displacement on the cleft side in the lateral direction; however, the authors used 2D photographs for the evaluation of the asymmetric displacements only in the horizontal direction. The head posture was standardized when superimposing in 2D, which may result in measurement errors due to superimposition. Another study used video recording system to evaluate nasolabial appearance and movement of the perioral area (Morrant and Shaw, 1996). Assessment of movement in the scar and surrounding facial soft tissue was conducted based on subjective evaluation by a panel of the plastic surgeon, which can be biased by observers (Ritter et al., 2002; Trotman et al., 2007). As for an attempt to evaluate smiling in a quantitative manner as well as in a 3-D, 3-D movements were assessed using a video-based tracking system that captured movement of landmarks placed at

specific sites on the face during instructed maximum smile, cheek puff, lip purse, mouth opening, and natural smile (Trotman et al., 2007). The landmark reflectors with 2-mm diameter located on the upper lip showed less movements in patients with CL±P when compared with the control group. Because the authors employed landmarks for the movement tracking, the displacements of the entire facial surface was still not clear.

On the other hand, the three-dimensional digital camera system has recently become a useful clinical tool for quantification of the facial surfaces. For example, 3D digital camera system has been widely used for evaluation of change in the nasal morphology after the maxillomandibular surgery (Honrado et al., 2006), evaluation of social smile reproducibility (Dindaroğlu et al., 2016), assessment of facial outcome following orthognathic treatment in patients with craniofacial syndrome (Claes et al., 2012), recognition of difference between patients with craniofacial syndrome with healthy controls (Hammond et al., 2004), and assessment of volumetric change from revision surgery in the cleft lip and palate nose (van Loon et al., 2010). In the present study, we employed 3D photographs at rest and at peak of the maximum smiling, and superimposition of these photographs enables us to understand the movements of the entire surface of the face during smiling in a quantitative manner.

Displacement of facial soft tissue during smiling

In the present study, the Cleft group showed greater lateral displacement and less upward and backward displacement on the scar area. This result indicates that scarring restricted anteroposterior and vertical motions but the lateral motions during smiling on the cleft side were not affected or even accelerated in the scar and surrounding facial soft tissue. The Cleft group also presented less lateral, upward, and backward displacement in the alar area on the non-cleft side. We assumed that there are mainly three possible factors to explain these impaired displacements of facial soft

tissue in patients with UCL±P as follows:

Firstly, tightened cleft scarring on the upper lip would be the causative factor of the asymmetric displacement. Scar formation is considered to be the product of collagen fiber synthesis and alignment, in the presence of a tensile stress field generated by a wound contraction process for a prior cleft (Yang et al., 2013). It is assumed that the tightened cleft scarring on the upper lip may have pulled the nose and the surrounding upper lip area towards the affected side while smiling, thereby causing asymmetric lateral displacement of the alar and upper lip area.

Secondly, the two functional components of the orbicularis oris muscle (i.e., the extrinsic and intrinsic bundles), which function as the retractor and constrictor of the mouth, respectively, were impaired even after the first repair surgery. Wijayaweera et al. (2000) revealed that the extrinsic bundles of orbicularis oris muscle were displaced and changed its direction by the cleft in patients with unilateral cleft lip. The extrinsic bundles are the retractor of orbicularis oris muscle and disfigurement of the extrinsic bundles may result in the asymmetric backward displacement of the scar area during smiling. There is a possibility that impaired muscle function could interrupt normal displacement of facial soft tissue.

Thirdly, there is a possibility that impaired perioral sensorimotor system in patients with UCL±P could affect displacement of facial soft tissue. A normal sensory function is necessary for the normal motor function of perioral area (Stranc et al., 1987; Essick, 1998). A previous study that assessed altered sensation areas by the interview showed the existence of the abnormal neurosensory function around a perioral area in patients CL±P (Essick et al., 2005). Evaluation of electromyography on the upper lip area also revealed the asymmetric distribution of muscle activity around cleft area, indicating impaired motor unit around cleft (Radeke et al., 2014). Impaired neurosensory and motor function in patients with UCL±P may result in disturbed

displacement of perioral area during smiling.

Asymmetric displacement of the cheek during smiling

In the present study, it was also found that there was an asymmetry of facial morphology in the cheek area where the Cleft group showed more retrusion on the non-cleft side than the cleft side at rest position (Appendix 3). As far as we know, this is the first study reporting asymmetry of prominence in the cheek area between cleft and non-cleft sides in patients with UCL±P. It is assumed that more retruded cheek area on the non-cleft side was related with less displacement of cheek on the non-cleft side during smiling. Greater downward displacement in the lower lip area with less upward displacement in the upper lip area was observed in the Cleft group. Trotman et al. (2000) reported in their study using a video-tracking system that greater displacement of the lower lip was observed with less displacement of the upper lip in patients with CLP. This can be interpreted as compensational movement of the lower lip for interrupted upper lip movements in patients with UCL±P.

Intermediate precision in the measurement of viscoelasticity

We evaluated the intermediate precision in the measurement of physical property in the present study. In general, there are three terms that represent the validity of the measurement method: repeatability, reproducibility, and intermediate precision. For repeatability to be established, all of the following conditions must be in place: the same location, measurement procedure, examiners, and instruments used under the same conditions, with repetition within a short period of time, such as 3 minutes (Murphy, 2010). Reproducibility conditions refer to the same method conducted on same test items in different laboratories, which necessarily involves different examiners and instrument, as well as differences in other factors such as laboratory environment,

management and even different interpretations of the test method itself (Murphy, 2010). Meanwhile, intermediate precision conditions allow for the varying of factors that could influence test method variation within a laboratory, including longer time periods such as weeks or months (Murphy, 2010). As for the repeatability of the viscoelasticity measuring instrument, a previous research has been reported as reliability in the measurement within a short period of time such as 3 minutes (Kuwahara et al., 2008). In clinical settings, intermediate precision with a longer period of time, such as weeks or months, is important when examining the changes induced by the clinical interventions. Thus, we examined intermediate precision in the measurement with an interval of a week in the present study.

Minimal detectable change

Measurement error is defined as the difference between a measured value of a quantity and its true value (Dodge, 2003). Minimal detectable change (MDC) is an absolute measure of reliability about measurement error, which is increasingly used to assist in interpreting results and determining whether a difference between repeated tests is a random error or a true change in measurement (Haley et al., 2006). Random error is unavoidable in measurement, which is caused by inherently unpredictable fluctuations in the readings of a measurement instrument or in the examiner's interpretation of the instrumental reading (Taylor, 1999). In this regard, it is necessary to evaluate factors which can affect the MDC in the measurement.

Factors which affect the precision of the measurement of physical property

There are mainly four factors which can affect the precision of the measurement of physical property. The first factor is the relocation of the instrument. A difference of MDC_{95} of viscoelasticity between landmarks was observed in the present

study. The least value of MDC_{95} of elastic modulus was found at *cheilion* (20.73 kN/m²) which approximated 43 % of the value of *cheek* (48.52 kN/m²), the greatest value of MDC_{95} of elastic modulus. These results indicated that precision of the measurements was site-specific. Likewise, the least value of MDC_{95} of viscosity coefficient was found at *cheilion* (80.04 N·s/m²) which approximated 47% of the value of *crista philitri inferior* (168.06 N·s/m²), the greatest value of MDC_{95} of viscosity coefficient. Our assumption about these results is that *cheilion* showed less value of MDC_{95} because it was relatively easier to relocate the instrument visually on the same position. The landmark of *cheek* was defined as `most prominent point of cheek`, however, it was difficult to coincide `most prominent point` perfectly in every measurement, which was considered to bring the relatively greater value of MDC_{95} at *cheek*. The landmark of *crista philtri inferior* is located on the vermilion border which is the junction of the lip with the surrounding facial skin on the exterior to the labial mucosa within the mouth (Mosby's Medical Dictionary, 2009). Because of the anatomical trait of the area where epidermis from highly keratinized external skin is changed to less keratinized internal skin, a small deviation in the relocation of the instrument might have brought relatively greater MDC_{95} at *crista philitri inferior*. Previous research about measuring physical properties of scars using the same instrument with the present study also indicated that relocation of the instrument was difficult (Niyaz et al., 2012). In short, relocation of the instrument was considered to affect the value of MDC_{95} in each landmark.

The second factor is precision of the instrument itself. Regarding the precision of the instrument, the previous study showed 6.05–10.32% of intra-examiner variability (Kuwahara, 2010). In our preliminary experiment, repeatability of elastic modulus and viscosity coefficient showed 4.14% and 3.13%, respectively, which is considered having adequate reliability. In this regard, precision of the instrument was considered reliable.

The third factor is laboratory environment. Previous research reported that skin

became stiffer with high temperature (50-80℃), however, there was no significant change of elastic modulus of skin in the range of 25-40℃ and viscosity of skin tissue was not affected by the change of temperature (Xu et al., 2008). In terms of humidity, skin became softened with an increase of moisture (Christensen et al., 1977). In the present study, room temperature was maintained to constant degree (25℃) and measurements were conducted on the evening of the clear day to diminish the effect of changes in temperature and humidity. It is shown that the factor of laboratory environment was well-controlled in the present study.

Finally, tension on the muscular tissue under the nasolabial facial soft tissue in the participant during the measurement can also affect viscoelasticity of facial soft tissue. There is orbicularis oris muscle underneath the landmark of *crista philitri superior, crista philitri inferior, and cheilion* whereas zygomaticus major muscle is located underneath the landmark of *cheek*. When the muscle is stretched, tension is developed within the muscle (Cooke and Holmes, 1986). Participants were vocally instructed to relax before the measurement and when participants had tension in the perioral area, measurements were repeated to exclude the effect from tension of the muscle. In this regard, the effect from tension of perioral muscle can be disregarded in the present study.

Comparison of viscoelasticity between the Cleft group and the Control group

To the best of our knowledge, the present study is the first attempt to measure the physical property of scar tissue and surrounding facial soft tissue in patients with UCL±P using viscoelasticity measuring instrument. In the present study, we determined only greater elastic modulus in the Cleft group than the Control group at the *crista philtri superior'* on the cleft side. However, because we observed the greater

variation of the physical properties in the Cleft group than in the Control group, we subcategorized the Cleft group into three sub-groups in the Experiment 4, which enabled us to understand detailed relationships between 3D displacements and the facial physical properties.

Relationship between viscoelasticity and displacement of facial soft tissue

The Cleft group was subcategorized into three subgroups and each subgroup showed characteristic physical property and displacement of facial soft tissue during smiling in the present study. A subgroup with less viscoelasticity (Code 1) showed relatively greater displacement during smiling in three directions. This result indicates that less viscoelasticity of the scar and surrounding facial soft tissue led to greater displacement of facial soft tissue. Code 1 also showed significantly greater elastic modulus at *crista philtri superior'* on the cleft side than the non-cleft side and greater lateral displacement in the scar area during smiling. Greater elastic modulus at the scar might have affected asymmetric lateral displacement of facial soft tissue around the scar.

A subgroup with the intermediate character of viscoelasticity (Code 2) between other two subgroups showed symmetric displacement of facial soft tissue in three directions. There was no significant difference of elastic modulus at *crista philtri superior'* between cleft and non-cleft side in this subgroup and this may affect the symmetric appearance of facial displacement. There was significant upward displacement in the nasal dorsum area and downward displacement in the lower lip and chin areas. Previous research indicated that downward displacement of the lower lip during smiling was related with the displacement of lower jaw in their discussion (Trotman et al., 2007). However, in the present study, participants were instructed to smile with the teeth in light contact in the habitual maximum intercuspation position. Therefore, it is considered that

there was no effect of the movement of lower jaw on the displacement of lower lip area. Thus we assumed that the downward displacement of the lower lip during smiling in the Cleft group is a compensatory movement for less movement of the upper lip during smiling.

A subgroup with greater and asymmetric viscoelasticity at the scar (Code 3) showed less lateral displacement in the cheek area on the non-cleft side and greater lateral displacement in the subalar area on the cleft side. There was restricted displacement of facial soft tissue in upward and backward directions. Increased elastic modulus at the scar in Code 3 seems to affect the smaller displacement of the facial soft tissue.

In the Experiment 1, the Cleft group showed greater lateral displacement in the scar area than the Control group. The Experiment 4 revealed this result was due to patients who were subcategorized into Codes 1 and 3 of the Cleft group. Asymmetric viscoelasticity between cleft and non-cleft side may result in the asymmetric displacement of facial soft tissue in patients with UCL±P. Likewise, in the Experiment 1, the Cleft group showed greater upward displacement in the nasal dorsum area and downward displacement in the lower lip area when compared with the Control group. Experiment 3 revealed that this downward movement of the lower lip in the Cleft group was due to patients who were categorized as the Code 2. It is assumed that symmetric viscoelasticity at *crista philtri superior'* between cleft and non-cleft side could result in free of asymmetric tensile stress around scar and might have allowed greater displacement of the nose and lower lip area. Overall, there was specific character of displacement in each subgroup and greater viscoelasticity at the scar was related with restricted displacement of facial soft tissue in three directions.

Clinical applications

Various treatment options have been reported to improve scar tissue, e.g., Er:YAG laser (Nocini et al., 2003), silicone gel sheet (Kim et al., 2014), and massage therapy; (McKay, 2014). Lip revision surgery and orthodontic/orthognathic treatment can also affect physical property of the scar and surrounding facial soft tissues. The best treatment option for improvement of facial motion function will be sought out by combining examinations of the 3D facial morphology and the physical properties of facial soft tissues in clinical settings.

Limitations

Our study has two limitations. Firstly, the sample size for analysis of effect from skeletal parameter on facial displacement was relatively small; therefore, it is possible that our results would have differed with a larger sample. Secondly, our sample population had limited variation in age (15–37 years) and in ethnicity (Japanese). Therefore, the readers should consider these sample variations when applying our findings to a different population.

CONCLUSION

It was found that physical properties of the scar and surrounding facial soft tissue affected 3D displacement of facial soft tissue during smiling in patients with repaired unilateral cleft lip with or without palate.

ACKNOWLEDGEMENTS

Firstly, I would like to express my sincere gratitude to my supervisor Prof. Takashi Yamashiro, Chairman of the Department of Orthodontics and Dentofacial Orthopedics, for the continuous support of my Ph.D. study, for his patience, motivation, and immense knowledge. His guidance helped me in all the time of research and writing of this thesis. I could not have imagined having a better supervisor and mentor for my Ph.D. study.

I also would like to thank my advisor Dr. Chihiro Tanikawa, Associate Professor of the Department of Orthodontics and Dentofacial Orthopedics, for providing me extensive professional guidance and teaching me a great deal about scientific research. Without her guidance and persistent help, this thesis would not have been possible.

Besides my advisors, I would like to thank my thesis committee: Prof. Atsushi Yoshida, Chairman of the Second Department of Oral Anatomy, Dr. Kanji Nohara, Associate Professor of the Department of Oral-Facial Disorders, and Dr. Susumu Tanaka, Associate Professor of the First Department of Oral and Maxillofacial Surgery, for their encouragement, insightful comments, and hard questions.

I would like to show my appreciation to all the faculty members and fellow students of the Department of Orthodontics and Dentofacial Orthopedics, for their help, cooperation, and encouragement for this research. I would like to offer my special thanks to Dr. Hiroshi Kurosaka, Associate Professor of the Department of Orthodontics and Dentofacial Orthopedics, for his valuable suggestions and kind encouragement during my Ph.D. study.

Nobody has been more important to me in the pursuit of this research than the members of my family. I would like to thank my parents, whose love and guidance are

always with me in wherever I am. I also thank my brother for his love and encouragement. Most importantly, I wish to thank my loving and supportive wife, Nari, and my wonderful son, Junsu, who provided inspiration and motivation for this research.

REFERENCES

Ackerman, J. L., Ackerman, M. B., Brensinger, C. M., & Landis, J. R. (1998). A morphometric analysis of the posed smile. Clinical Orthodontics and Research, 1998;1:2–11.

Barlow, S. M., Trotman, C. A., Chu, S. Y., & Lee, J. (2012). Modification of perioral stiffness in patients with repaired cleft lip and palate. Cleft Palate-craniofacial Journal, 49(5), 524–529.

Bland, J. M., & Altman, D. (1986). Statistical methods for assessing agreement between two methods of clinical measurement. The Lancet, 327(8476), 307–310.

Christensen, M. S., Hargens, C. W., Nacht, S., & Gans, E. H. (1977). Viscoelastic properties of intact human skin: instrumentation, hydration effects, and the contribution of the stratum corneum. Journal of Investigative Dermatology, 69(3), 282-286.

Claes, P., Walters, M., & Clement, J. (2012). Improved facial outcome assessment using a 3D anthropometric mask. International journal of oral and maxillofacial surgery, 41(3), 324–330.

Cooke, R. & Holmes, K. C. (1986). The mechanism of muscle contraction. Critical

Reviews in Biochemistry, 21:1, 53–118.

Corr, D. T., Gallant-Behm, C. L., Shrive, N. G., & Hart, D. A. (2009). Biomechanical behavior of scar tissue and uninjured skin in a porcine model. Wound Repair and Regeneration, 17(2), 250–259.

Dindaroğlu, F., Duran, G. S., Görgülü, S., & Yetkiner, E. (2016). Social smile reproducibility using 3-D stereophotogrammetry and reverse engineering technology. The Angle Orthodontist, 86(3), 448–455.

Dodge, Y. (2003). The Oxford Dictionary of Statistical Terms, OUP.

Dunn, M. G., Silver, F. H., & Swann, D. A. (1985). Mechanical analysis of hypertrophic scar tissue: Structural basis for apparent increased rigidity. Journal of Investigative Dermatology, 84(1), 9–13.

Essick, G. K. (1998). Effects of hypesthesia on oral behaviors of the orthognathic surgery patient. Journal of Oral and Maxillofacial Surgery, 56(2), 158–160.

Essick, G. K., Dorion, C., Rumley, S., Rogers, L., Young, M., & Trotman, C. A. (2005). Report of altered sensation in patients with cleft lip. Cleft palate-craniofacial journal, 42(2), 178–184.

Essick, G. K., Phillips, C., & Trotman, C. A. (2007). Functional outcomes of cleft lip surgery. Part IV: Between- and within-participant variables affecting lip vermilion sensory thresholds. Cleft Palate-craniofacial Journal, 44(6), 624–634.

Gonzalez, P. N., Bernal, V., & Perez, S. I. (2011). Analysis of sexual dimorphism of craniofacial traits using geometric morphometric techniques. International Journal of Osteoarchaeology, 21(1), 82–91.

Haley S. M., & Fragala-Pinkham M.A. (2006). Interpreting change scores of tests and measures used in physical therapy. Physical Therapy, 86:735–743.

Hammond, P., Hutton, T. J., Allanson, J. E., Campbell, L. E., Hennekam, R., Holden, S., & Murphy, K. C. (2004). 3D analysis of facial morphology. American Journal of Medical Genetics Part A, 126(4), 339–348.

Honrado, C. P., Lee, S., Bloomquist, D. S., & Larrabee, W. F. (2006). Quantitative assessment of nasal changes after maxillomandibular surgery using a 3-dimensional digital imaging system. Archives of Facial Plastic Surgery, 8(1), 26.

Kim, S. M., Choi, J. S., Lee, J. H., Kim, Y. J., & Jun, Y. J. (2014). Prevention of postsurgical scars: comparison of efficacy and convenience between silicone gel sheet and topical silicone gel. Journal of Korean Medical Science, 29 (Suppl 3), S249–S253.

Kono, K., Tanikawa, C., Yanagita, T., Kamioka, H., & Yamashiro, T. (2017). A Novel Method to detect 3D mandibular changes related to soft-diet feeding. Frontiers in Physiology, 8, 567.

Kuwahara, Y., Shima, Y., Shirayama, D., Kawai, M., Hagihara, K., Hirano, T., & Kawase,

I. (2008). Quantification of hardness, elasticity and viscosity of the skin of patients with systemic sclerosis using a novel sensing device (Vesmeter): a proposal for a new outcome measurement procedure. Rheumatology, 47(7), 1018–1024.

Lane, C., & Harrell, W. (2008). Completing the 3-dimensional picture. American Journal of Orthodontics and Dentofacial Orthopedics, 133(4), 612–620.

Lübbers, H. T., Medinger, L., Kruse, A., Grätz, K. W., & Matthews, F. (2010). Precision and accuracy of the 3dMD photogrammetric system in craniomaxillofacial application. Journal of Craniofacial Surgery, 21(3), 763–767.

MacQueen, J. (1967). Some methods for classification and analysis of multivariate observations. In Proceedings of the Fifth Berkeley Symposium on Mathematical Statistics and Probability, 1(14), 281–297.

McKay, E. (2014). Assessing the effectiveness of massage therapy for bilateral cleft lip reconstruction scars. International Journal of Therapeutic Massage & Bodywork, 7(2), 3.

Millar, K., Bell, A., Bowman, A., Brown, D., Lo, T. W., Siebert, Paul, S., Simmons, D., & Ayoub, A. (2013). Psychological status as a function of residual scarring and facial asymmetry after surgical repair of cleft lip and palate. Cleft Palate-craniofacial Journal, 50(2), 150–157.

Morrant, D. G., & Shaw, W. C. (1996). Use of standardized video recordings to assess cleft surgery outcome. Cleft palate-craniofacial Journal, 33(2), 134–142.

Mosby's Medical Dictionary, 8th edition. "vermilion border. https://medical-dictionary.thefreedictionary.com/vermilion+border. Retrieved December 25, 2017.

Mulliken, J. B., Burvin, R., & Farkas, L. G. (2001). Repair of bilateral complete cleft lip: intraoperative nasolabial anthropometry. Plastic and reconstructive surgery, 107(2), 307-314.

Murphy, T. (2010). American Society for Testing and Materials International. https://www.astm.org/SNEWS/ND_2010/datapoints_nd10.html. Retrieved December 21, 2017.

Niyaz, A., Matsumura, H., Watanabe, K., Hamamoto, T., & Matsusawa, T. (2012). Quantification of the physical properties of keloid and hypertrophic scars using the Vesmeter novel sensing device. International Wound Journal, 9(6), 643–649.

Nocini, P. F., D'Agostino, A., Trevisiol, L., & Bertossi, D. (2003). Treatment of scars with Er: YAG laser in patients with cleft lip: a preliminary report. Cleft Palate-craniofacial Journal, 40(5), 518–522.

Offerman, R. E., Cleall, J. F., & Subtelny, J. D. (1964). Symmetry of lip activity in repaired unilateral clefts of the lip. Cleft Palate Journal, 1(3), 347–356.

Radeke, J., van Dijk, J. P., Holobar, A., & Lapatki, B. G. (2014). Electrophysiological method to examine muscle fiber architecture in the upper lip in cleft-lip patients.

Journal of Orofacial Orthopedics / Fortschritte Der Kieferorthopädie, 75(1), 51–61.

Ritter, K., Trotman, C. A., & Phillips, C. (2002). Validity of subjective evaluations for the assessment of lip scarring and impairment. Cleft Palate-craniofacial Journal, 39(6), 587–596.

Stranc, M. F., Fogel, M., & Dische, S. (1987). Comparison of lip function: surgery vs radiotherapy. British Journal of Plastic Surgery, 40(6), 598–604.

Tanikawa, C., Kakiuchi, Y., Yagi, M., Miyata, K., & Takada, K. (2007). Knowledge-dependent pattern classification of human nasal profiles. The Angle Orthodontist, 77(5), 821–830.

Tanikawa, C., Takada, K., Van Aalst, J., & Trotman, C. A. (2010). Objective three-dimensional assessment of lip form in patients with repaired cleft lip. Cleft Palate-craniofacial Journal, 47(6), 611–622.

Tanikawa. C & Takada K. (2017). Test re-test reliability of smile tasks using three-dimensional facial topography. The Angle Orthodontist, in press.

Taylor, J. R. (1999) An Introduction to Error Analysis: The study of uncertainties in physical measurements, University Science Books, ISBN: 093570275X, p. 94, §4.1.

Trotman, C. A., Faraway, J. J., & Essick, G. K. (2000). Three-dimensional nasolabial displacement during movement in repaired cleft lip and palate patients. Plastic

and Reconstructive Surgery, 105(4), 1273–1283.

Trotman, C. A., Phillips, C., Essick, G. K., Faraway, J. J., Barlow, S. M., Losken, H. W., ... & Rogers, L. (2007). Functional outcomes of cleft lip surgery. Part I: study design and surgeon ratings of lip disability and need for lip revision. Cleft Palate-craniofacial Journal, 44(6), 598–606.

Trotman, C. A., Faraway, J. J., Losken, H. W., & Van Aalst, J. A. (2007). Functional outcomes of cleft lip surgery. Part II: Quantification of nasolabial movement. Cleft Palate-craniofacial Journal, 44(6), 607–616.

Turner, S., Rumsey, N., & Sandy, J. (1998). Psychological aspects of cleft lip and palate. European Journal of Orthodontics, 20(4), 407–416.

Van Loon, B., Maal, T. J., Plooij, J. M., Ingels, K. J., Borstlap, W. A., Kuijpers-Jagtman, A. M., ... & Berge, S. J. (2010). 3D Stereophotogrammetric assessment of pre-and postoperative volumetric changes in the cleft lip and palate nose. International Journal of Oral and Maxillofacial Surgery, 39(6), 534–540.

Wijayaweera, C. J., Amaratunga, N. A., & Angunawela, P. (2000).Arrangement of the orbicularis oris muscle in different types of cleft lips. Journal of Craniofacial Surgery, 11:232–235.

Xu, F., Seffen, K. A., & Lu, T. J. (2008). Temperature-dependent mechanical behaviors of skin tissue. IAENG International Journal of Computer Science, 35(1).

Yang, L., Witten, T. M., & Pidaparti, R. M. (2013). A biomechanical model of wound contraction and scar formation. Journal of Theoretical Biology, 332:228–248.

Wada, K. (1977). A study on the individual growth of maxillofacial skeleton by means of lateral cephalometric roentgenograms. Journal of Osaka University Dental School, 22, 239-269.

FIGURE LEGENDS

Figure 1: 3D image acquisition. Black arrows: three-dimensional image capturing device (3dMDcranial System, 3dMD, Atlanta, GA, USA).

Figure 2: 3D coordinate system. The nasion (N) was defined as the origin (O). The sagittal plane was defined as a plane passing through the origin and perpendicular to the line through the midpoint of the right exocanthion (Ex) and endocanthion (En) and the midpoint of the left Ex and En. The axial plane was defined as a plane passing through the origin and parallel to the line connecting the porion and the geometric center (g) of porion (Po), subnasale (Sn), and Ex on the image projected onto the sagittal reference plane. The coronal plane was defined as a plane passing through the origin and perpendicular to both the axial and the sagittal planes.

Figure 3: Standardization of the facial image at the peak of posed smiling with the Iterative Closest Point algorithm.

Figure 4: The mesh fitting method of 3D image. For each facial model, fitting of template meshes was performed using software, based on the landmarks. This method automatically generated a homogeneous model consisting of 6,017 points on the wire mesh for each model.

Figure 5: Schematic illustration of computation and visualization of averaged face (Ave, Average; SD, Standard deviation).

Figure 6: Schematic illustration of statistical comparison of displacement from rest posture to the peak of the maximum smile posture between the Control group and the Cleft group (R_{ctl}, Rest of the Control group; S_{ctl}, Smile of the Control group; R_{clt}, Rest of the Cleft group; S_{clt}, Smile of the Cleft group).

Figure 7: Landmarks employed in the present study (A), measurement of viscoelasticity in the facial soft tissue with viscoelasticity measuring instrument (B), and indenter of viscoelasticity measuring instrument (C).
Chk indicates *cheek*; *Cphs'*, *crista philtri superior'*; *Cphi*, *crista philtri inferior*; *Ch*, *cheilion*; L, cleft side; R, right side. Black arrow in (B): Probe of viscoelasticity measuring instrument (Vesmeter-E100Hs, WaveCyber Corp., Saitama, Japan). Black arrow in (C): Indenter of viscoelasticity measuring instrument.

Figure 8: Significance probability maps (top) and distant maps (bottom) of the difference of displacement during smiling between the Control Group and the Cleft group in three directions (horizontal, vertical, and anteroposterior directions). For the significance probability maps, Blue designates $P \leq 0.05$; Pale pink, $P \leq 0.01$; Dark pink, $P \leq 0.001$; Purple, $P \leq 0.0001$. For the distance maps, Red indicates that difference of displacement between two subject groups (Control group - Cleft group) is a positive value whereas Blue indicates that difference of displacement between two subject groups (Control group - Cleft group) is a negative value.

Figure 9: Comparison of elastic modulus between the Cleft group and the Control group.

Figure 10: Comparison of viscosity coefficient between the Cleft group and the Control

group.

Figure 11: Comparison of elastic modulus and viscosity coefficient between each Code. A: Comparison of elastic modulus between each Code; B: Comparison of viscosity coefficient between each Code. *Chk* indicates *cheek*; *Cphs'*, *crista philtri superior'*; *Cphi*, *crista philtri inferior*; *Ch*, *cheilion*;

Figure 12: Significance probability maps (first, third, and fifth from top) and distant maps (second, fourth, and sixth from top) of the difference of displacement during smiling in each Code in three directions (horizontal, vertical, and anteroposterior directions). For the significance probability maps, Blue designates $P \leq 0.05$; Pale pink, $P \leq 0.01$; Dark pink, $P \leq 0.001$; Purple, $P \leq 0.0001$. For the distance maps, Red indicates that difference of displacement between two subject groups (Control group - Cleft group) is a positive value whereas Blue indicates that difference of displacement between two subject groups (Control group - Cleft group) is a negative value.

Supplementary Figure 1: Significance probability maps (top) and distant maps (bottom) of the mean difference between the Control Group and the Cleft group for each facial expression. For the images on the upper side, the pink color indicates greater P values. A: Comparison between the Control group and Cleft group in rest posture; B: Comparison between the Control group and Cleft group in the smiling.

Table 1 Definition of tasks

Task	Definition
Rest	After swallowing saliva, subjects assumed a relaxed facial posture with the lips in repose and the teeth in light contact in the habitual maximum intercuspation position. The recording was made approximately 10 seconds after commencement of the saliva swallowing.
Peak of the maximum smile	A grinning effort was conducted with the corners of the mouth pulled laterally and the cheeks elevated with a maximal effort and with the teeth in the habitual maximum intercuspation position.

Table 2 Comparison of displacement during smiling between two groups on the non-cleft side

Area	Lateral – direction (X-value)	Upward - direction (Y-value)	Downward - direction (Y-value)	Backward – direction (Z-value)
Cheek	**** Cleft < Control	**** Cleft < Control	NS	*** Cleft < Control
Nasal - dorsum	NS	** Cleft < Control	NS	* Cleft < Control
Alar	** Cleft < Control	** Cleft < Control	NS	* Cleft < Control
Subalar	NS	NS	NS	NS
Upper lip	NS	*** Cleft < Control	NS	** Cleft < Control
Labial - commissure	NS	** Cleft < Control	NS	* Cleft < Control
Lower lip	NS	NS	** Cleft>Control	NS

****, P < 0.0001; ***, P < 0.001; **, P < 0.01; *, P < 0.05; NS : Not significant

'Cleft > Control' indicates that the Cleft group showed significantly greater averaged displacements when compared with the Control group; 'Cleft < Control', the Control group showed significantly greater averaged displacements when compared with the Cleft group.

Table 3 Comparison of displacement during smiling between two groups on the cleft side

Area	Lateral – direction (X-value)	Upward – direction (Y-value)	Downward – direction (Y-value)	Backward – direction (Z-value)
Cheek	NS	** Cleft < Control	NS	NS
Nasal - dorsum	NS	NS	NS	* Cleft < Control
Alar	NS	NS	NS	* Cleft < Control
Subalar	* Cleft > Control	NS	NS	* Cleft < Control
Upper lip	NS	* Cleft < Control	NS	**** Cleft < Control
Labial – commissure	NS	** Cleft < Control	NS	** Cleft < Control
Lower lip	NS	NS	** Cleft > Control	NS

****, P < 0.0001; ***, P < 0.001; **, P < 0.01; *, P < 0.05; NS : Not significant

'Cleft > Control' indicates that the Cleft group showed significantly greater averaged displacements when compared with the Control group; 'Cleft < Control', the Control group showed significantly greater averaged displacements when compared with the Cleft group.

Table 4 The mean and standard deviation (S.D.) of the minimal detectable change for each landmark at the 95% confidence level (MDC_{95}) between Session 1 and Session 2

Landmark	Elastic modulus (kN/m^2)	Viscosity coefficient ($N \cdot s/m^2$)
	Mean ± S.D.	Mean ± S.D.
Chk (Left)	48.5 ± 24.8	111.4 ± 56.8
Cphs' (Left)	43.2 ± 22.1	149.8 ± 76.4
Cphi (Left)	45.1 ± 23.0	168.1 ± 85.7
Ch (Left)	20.7 ± 10.6	80.0 ± 40.8
Overall	39.4 ± 12.6	127.3 ± 39.4

Chk: *cheek; Cphs'*: *crista philtri superior'; Cphi*: *crista philtri inferior; Ch*: *cheilion*.

Table 5 The mean and standard deviation (S.D.) of dental and skeletal parameters in each Code

Parameter	Code 1	Code 2	Code 3	
	Mean ± S.D.	Mean ± S.D.	Mean ± S.D.	P value
SNA (°)	75.5 ± 4.4	74.0 ± 5.6	74.4 ± 1.8	0.430
SNB (°)	76.3 ± 6.1	75.1 ± 5.7	75.9 ± 3.0	0.742
ANB (°)	-0.8 ± 5.0	-1.1 ± 3.2	-1.5 ± 2.4	0.663
SNMP (°)	39.3 ± 7.9	37.0 ± 8.4	38.8 ± 8.1	0.689
SNPP (°)	11.4 ± 5.7	13.9 ± 6.9	14.2 ± 5.3	0.215
N-Me (mm)	130.1 ± 8.7	129.0 ± 7.1	132.6 ± 10.2	0.669
Me/PP (mm)	72.2 ± 6.4	72.1 ± 6.0	71.5 ± 4.6	0.811
Ar-Go (mm)	46.6 ± 7.6	48.6 ± 5.0	47.1 ± 8.5	0.674
Ar-Me (mm)	108.4 ± 9.7	109.1 ± 8.6	111.7 ± 8.2	0.435
A-Ptm/PP (mm)	44.2 ± 4.7	44.3 ± 4.6	46.5 ± 3.5	0.332
A-McNamara (mm)	-8.0 ± 4.9	-9.1 ± 6.1	-8.8 ± 3.4	0.601
OJ (mm)	-0.1 ± 5.3	0.8 ± 3.5	-1.6 ± 3.4	0.638
OB (mm)	1.1 ± 2.9	0.5 ± 1.9	-0.4 ± 1.5	0.169

SNA: S-N-A angle; SNB: S-N-B angle; ANB: A-N-B angle; SNMP: The angle formed by the SN plane and the mandibular plane (Go-Me); SNPP: The angle formed by the SN plane and the palatal plane; N-Me: Total anterior facial height; Me/PP: Lower anterior facial height; Ar-Go: Ramus length; Ar-Me: Mandibular length; A-Ptm/PP: Point A to Ptm distance projected on the palatal plane (ANS-PNS); A-McNamara: The distance from Point A to the McNamara line, defined as a line perpendicular to the FH plane (Or-Po) and passing thorough the N; OJ: Overjet; OB: Overbite.

Table 6 Displacement during smiling in each Code in the horizontal direction (X-axis)

	Code 1		Code 2		Code 3	
Physical property	Less viscoelasticity, asymmetric		Intermediate character between Codes 1 and 3, symmetric		Greater viscoelasticity at the scar, more asymmetric	
Side	Cleft	Non-cleft	Cleft	Non-cleft	Cleft	Non-cleft
Cheek	****	****	**	**	****	*
Nasal – dorsum	NS	NS	NS	NS	NS	NS
Alar	*	*	*	*	*	*
Subalar	***	**	**	**	**	*
Upper lip	*	*	*	*	*	*
Labial – commissure	****	****	*	*	**	****
Lower lip	****	****	***	***	**	**

****, P < 0.0001; ***, P < 0.001; **, P < 0.01; *, P < 0.05; NS : Not significant

Table 7 Displacement during smiling in each Code in the vertical direction (Y-axis)

	Code 1		Code 2		Code 3	
Physical property	Less viscoelasticity, asymmetric		Intermediate character between Codes 1 and 3, symmetric		Greater viscoelasticity at the scar, more asymmetric	
Side	Cleft	Non-cleft	Cleft	Non-cleft	Cleft	Non-cleft
Cheek	**	**	**	**	NS	NS
Nasal – dorsum	NS	NS	*	*	NS	NS
Alar	*	*	***	***	NS	NS
Subalar	*	*	**	**	NS	NS
Upper lip	**	**	***	***	NS	NS
Labial – commissure	****	****	****	****	**	**
Lower lip	NS	NS	*	*	NS	NS

****, P < 0.0001; ***, P < 0.001; **, P < 0.01; *, P < 0.05; NS : Not significant

Table 8 Displacement during smiling in each Code in the anteroposterior direction (Z-axis)

	Code 1		Code 2		Code 3	
Physical property	Less viscoelasticity, asymmetric		Intermediate character between Codes 1 and 3, symmetric		Greater viscoelasticity at the scar, more asymmetric	
Side	Cleft	Non-cleft	Cleft	Non-cleft	Cleft	Non-cleft
Cheek	*	**	*	*	*	NS
Nasal – dorsum	NS	NS	NS	NS	NS	NS
Alar	*	*	*	*	NS	NS
Subalar	*	*	*	*	NS	*
Upper lip	****	****	****	****	NS	NS
Labial – commissure	****	****	****	****	**	****
Lower lip	***	***	**	**	*	**

****, P < 0.0001; ***, P < 0.001; **, P < 0.01; *, P < 0.05; NS : Not significant

Supplementary Table 1 Dental and skeletal parameters of the Cleft group

	Cleft group	Japanese Norm*	
	Mean ± S.D.	Mean ± S.D.	P value
SNA (°)	74.8 ± 4.5	81.5 ± 3.3	0.355
SNB (°)	75.8 ± 5.4	77.8 ± 4.0	0.266
ANB (°)	-1.0 ± 4.0	3.2 ± 2.4	0.452
SNMP (°)	38.4 ± 8.0	37.6 ± 6.1	0.099
SNPP (°)	12.8 ± 6.1	8.6 ± 2.2	0.071
N-Me (mm)	130.1 ± 8.3	135.7 ± 4.0	0.142
Me/PP (mm)	72.1 ± 5.8	74.6 ± 3.0	0.292
Ar-Go (mm)	47.4 ± 6.8	53.2 ± 5.7	0.142
Ar-Me (mm)	109.2 ± 8.9	115.6 ± 6.8	0.066
A-Ptm/PP (mm)	44.6 ± 4.5	51.3 ± 3.8	0.329
A-McNamara (mm)	-8.5 ± 5.1	2.5 ± 3.1	0.332
OJ (mm)	0.0 ± 4.4	3.3 ± 1.0	0.482
OB (mm)	0.6 ± 2.4	3.3 ± 1.7	0.630

* Wada et al. (1977)

SNA: S-N-A angle; SNB: S-N-B angle; ANB: A-N-B angle; SNMP: The angle formed by the SN plane and the mandibular plane (Go-Me); SNPP: The angle formed by the SN plane and the palatal plane; N-Me: Total anterior facial height; Me/PP: Lower anterior facial height; Ar-Go: Ramus length; Ar-Me: Mandibular length; A-Ptm/PP: Point A to Ptm distance projected on the palatal plane (ANS-PNS); A-McNamara: The distance from Point A to the McNamara line, defined as a line perpendicular to the FH plane (Or-Po) and passing thorough the N; OJ: Overjet; OB: Overbite.

APPENDIX 1

Given two 3D point sets, Prest and Psmile, the task is to find the Euclidean motion that brings Psmile into the best possible alignment with Prest. The Iterative Closest Point algorithm is consisted of three basic steps:

1. Pair each point of Psmile to the closest point in Prest

2. Compute the motion that minimizes the mean square error (MSE) between the paired points

3. Apply the motion to Psmile and update the MSE.

The three steps are iterated; the iterations have been proved to converge in terms of the MSE.

APPENDIX 2

A two-sample t-test was used to examine whether there as any significant difference in dental and skeletal parameters between the Cleft group and Japanese normal value (Wada et al., 1977). As a result, there was no significant difference of dental and skeletal parameters between the Cleft group and Japanese normal value (Please see Supplementary Table 1).

APPENDIX 3

Supplementary Figure 1 gives the average differences between the Control Group and the Cleft group and the significance probability map of the Z-values calculated for each facial posture.

Nose. The Cleft group showed significantly more retruded nasal tip area compared with the Control group at rest and during smiling by approximately 3.5 mm and 3mm, respectively ($P \leq 0.001$).

Cheek. The Cleft group showed significantly retruded cheek area on the non-cleft side when compared with the Control group at rest and during smiling by approximately 3.0mm ($P \leq 0.05$). However, there was no significant difference of facial morphology between the Cleft group and the Control group in the cheek area on the cleft side at rest and during smiling.

Upper lip. At rest, the Cleft group showed significantly more retruded upper lip area compared with the Control group by approximately 6.5 mm on average for both sides ($P \leq 0.001$). During smiling, the Cleft group showed significantly more retruded upper lip area compared with the Control group by approximately 4.5 mm on average for both sides ($P \leq 0.001$).

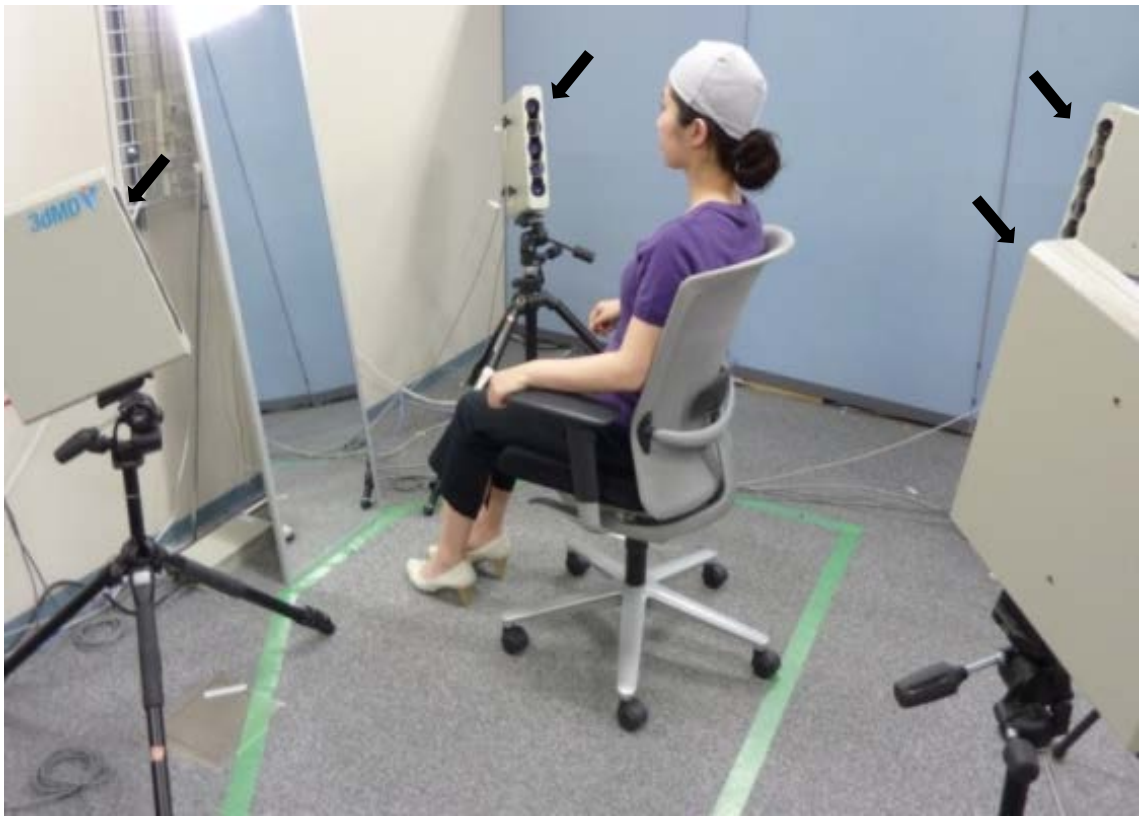

Figure 1

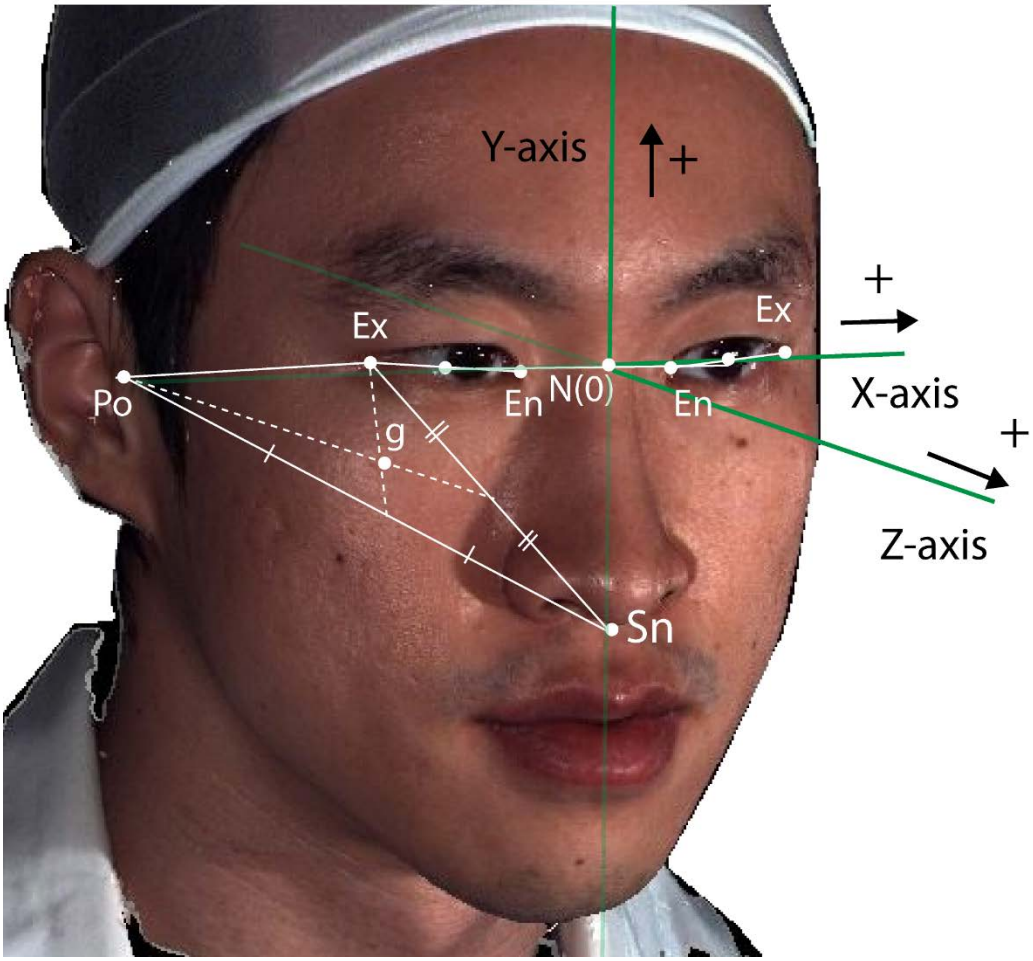

Figure 2

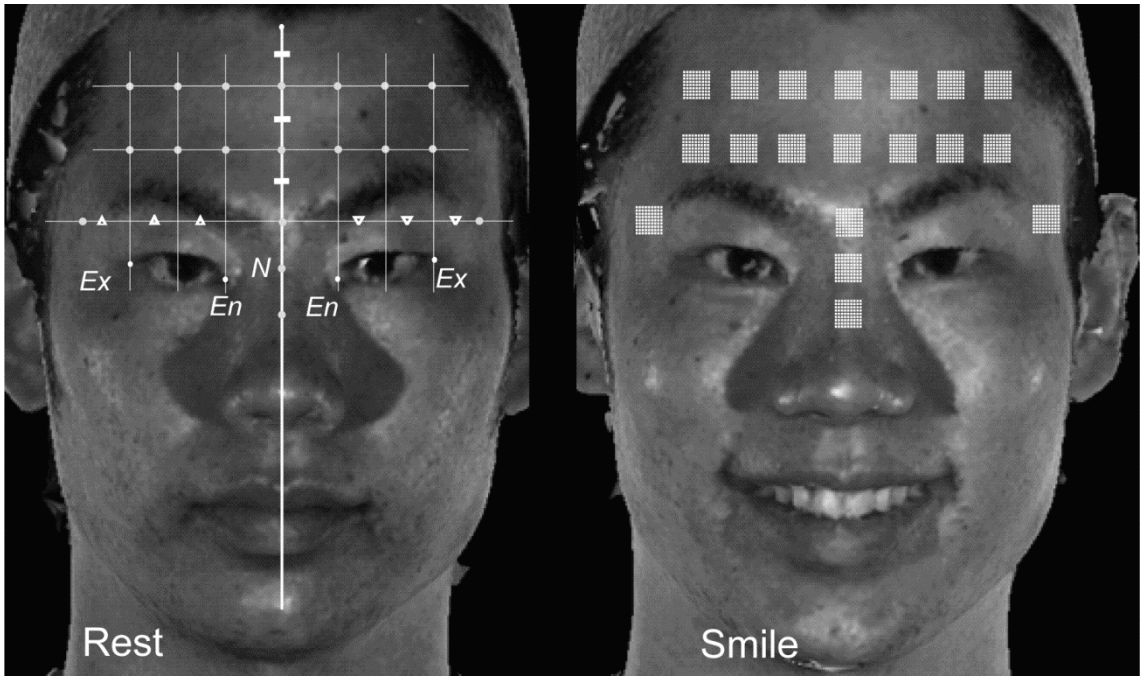

Figure 3

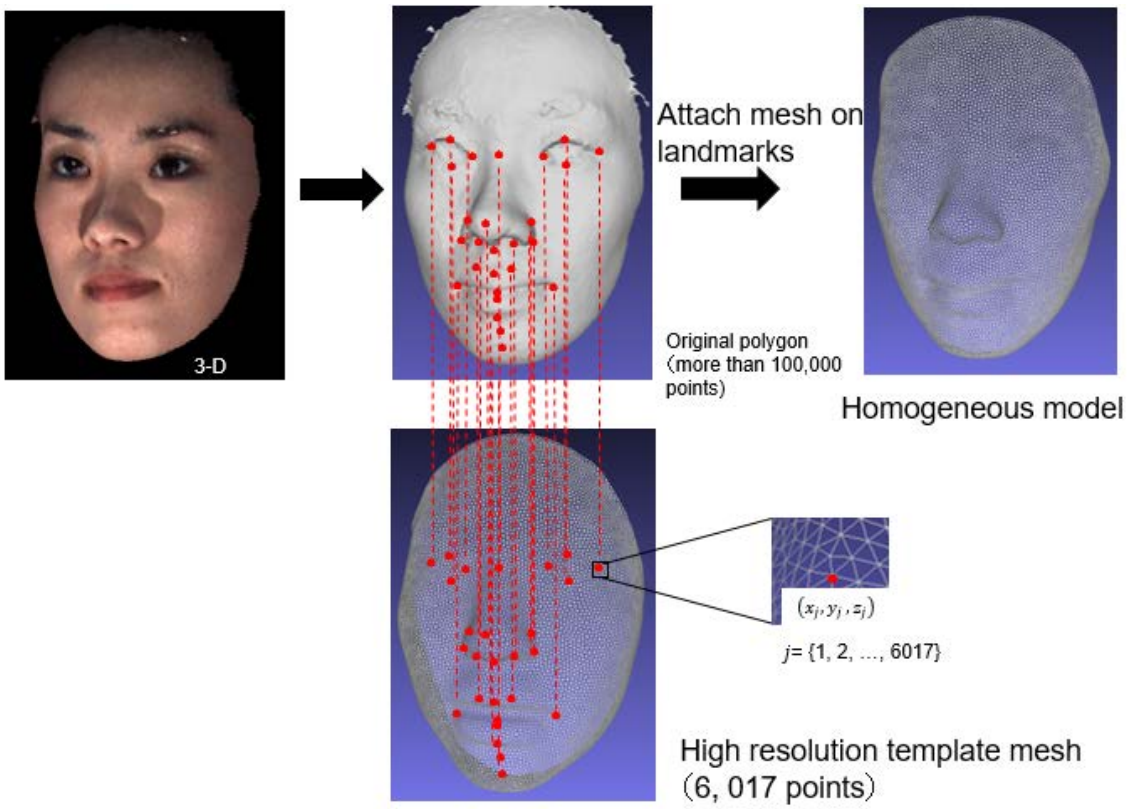
3-D
Attach mesh on landmarks
Original polygon (more than 100,000 points)
Homogeneous model
(x_j, y_j, z_j)
j= {1, 2, ..., 6017}
High resolution template mesh (6, 017 points)

Figure 4

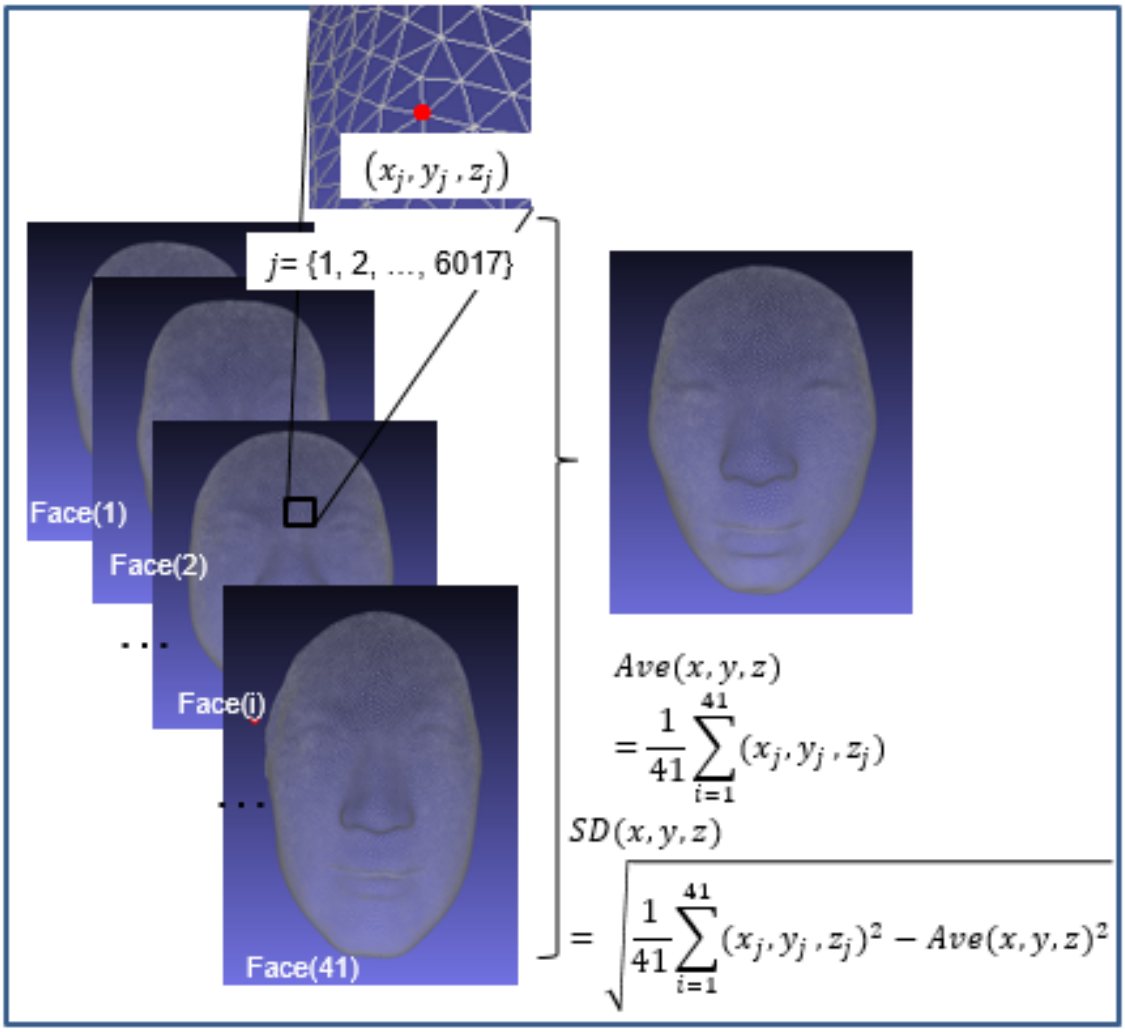
(x_j, y_j, z_j)
j= {1, 2, ..., 6017}
Face(1)
Face(2)
Face(i)
Face(41)
$Ave(x,y,z) = \frac{1}{41}\sum_{i=1}^{41}(x_j, y_j, z_j)$
$SD(x,y,z) = \sqrt{\frac{1}{41}\sum_{i=1}^{41}(x_j, y_j, z_j)^2 - Ave(x,y,z)^2}$

Figure 5

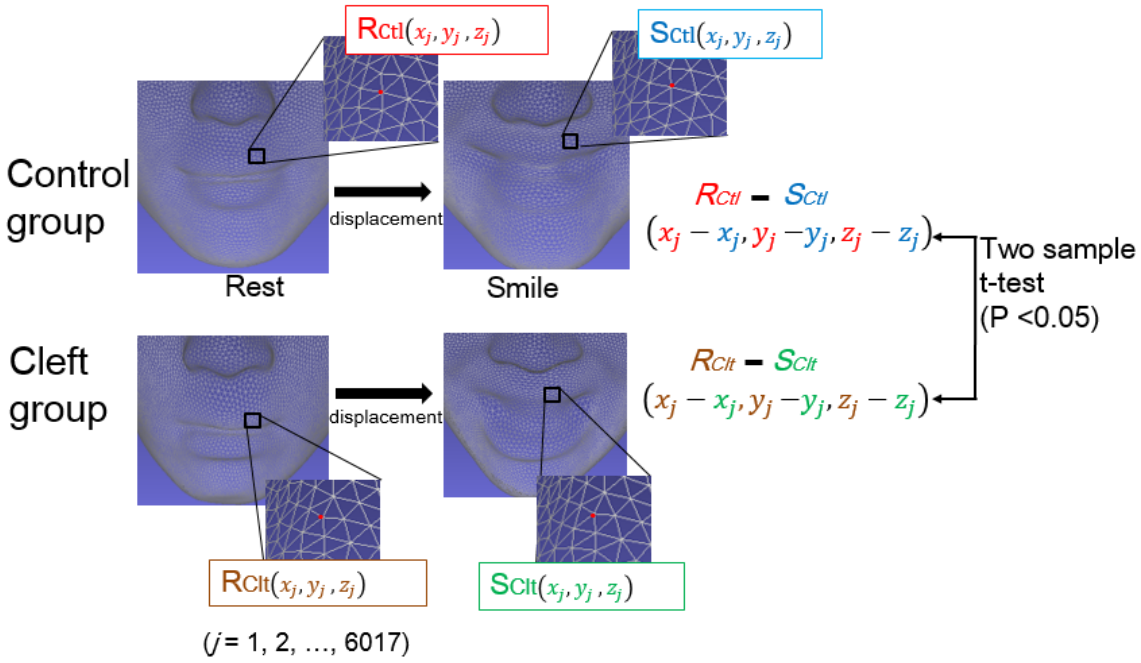
Control group
Cleft group
Rest
Smile
displacement
displacement
Two sample t-test (P <0.05)
(j = 1, 2, …, 6017)

Figure 6

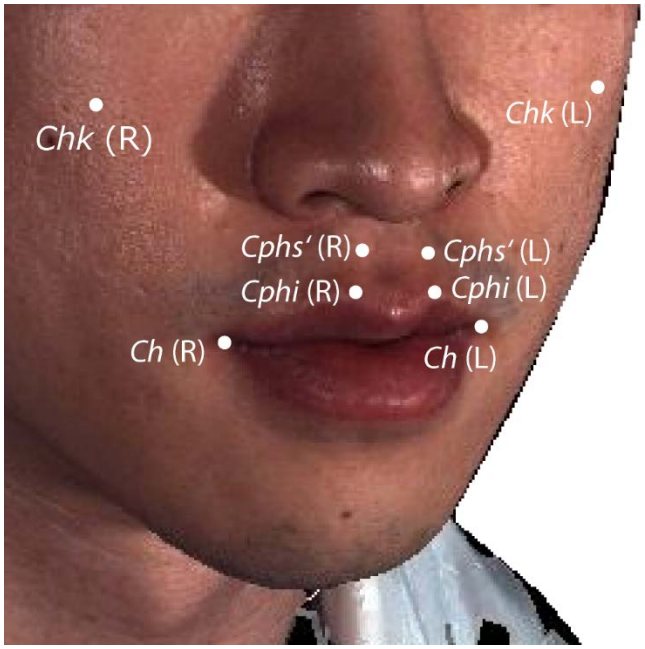

A

B

C

Figure 7

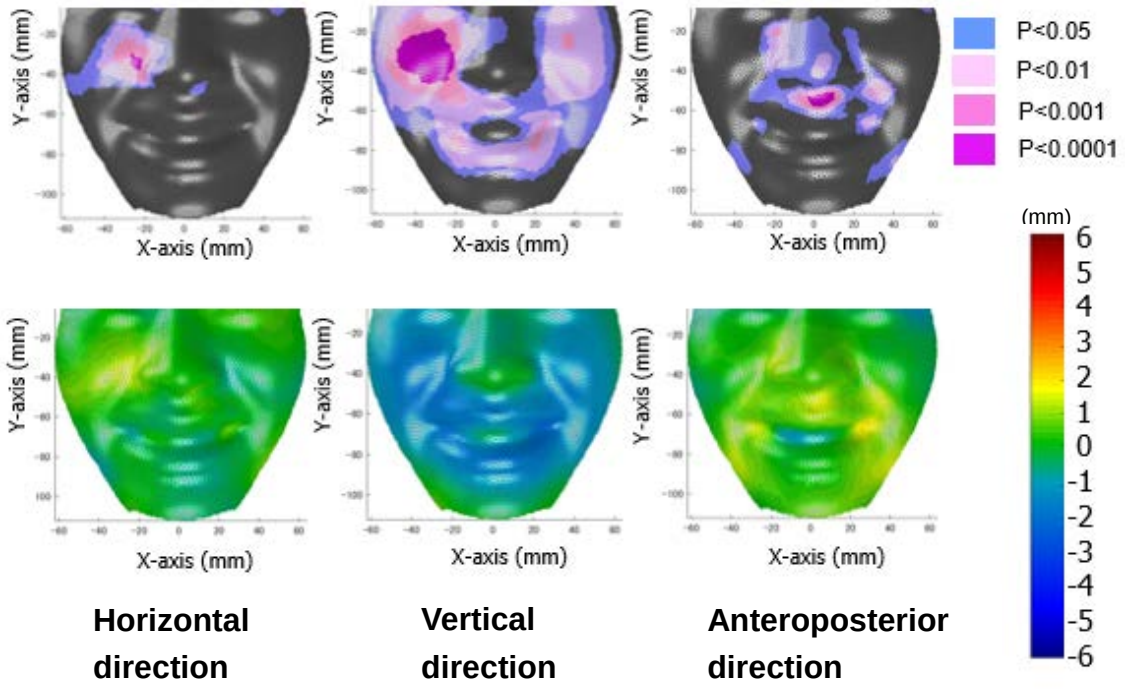
Y-axis (mm)
X-axis (mm)
P<0.05
P<0.01
P<0.001
P<0.0001
(mm)
6
5
4
3
2
1
0
-1
-2
-3
-4
-5
-6
Horizontal direction
Vertical direction
Anteroposterior direction

Figure 8

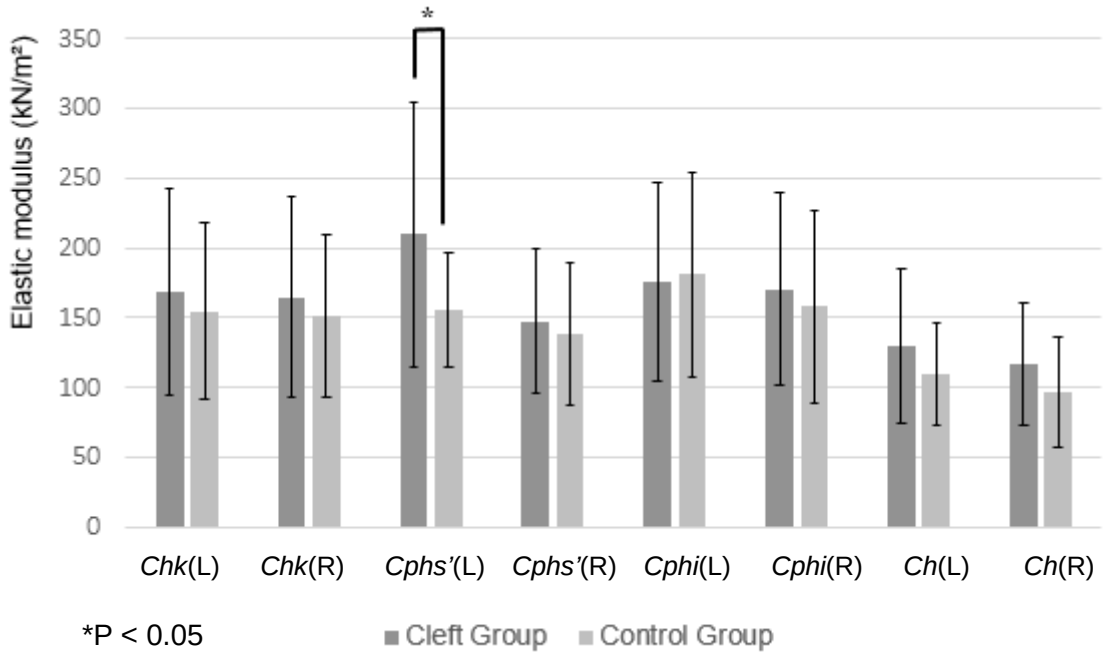
Elastic modulus (kN/m²)
350
300
250
200
150
100
50
0
*
Chk(L)
Chk(R)
Cphs'(L)
Cphs'(R)
Cphi(L)
Cphi(R)
Ch(L)
Ch(R)
*P < 0.05
Cleft Group
Control Group

Figure 9

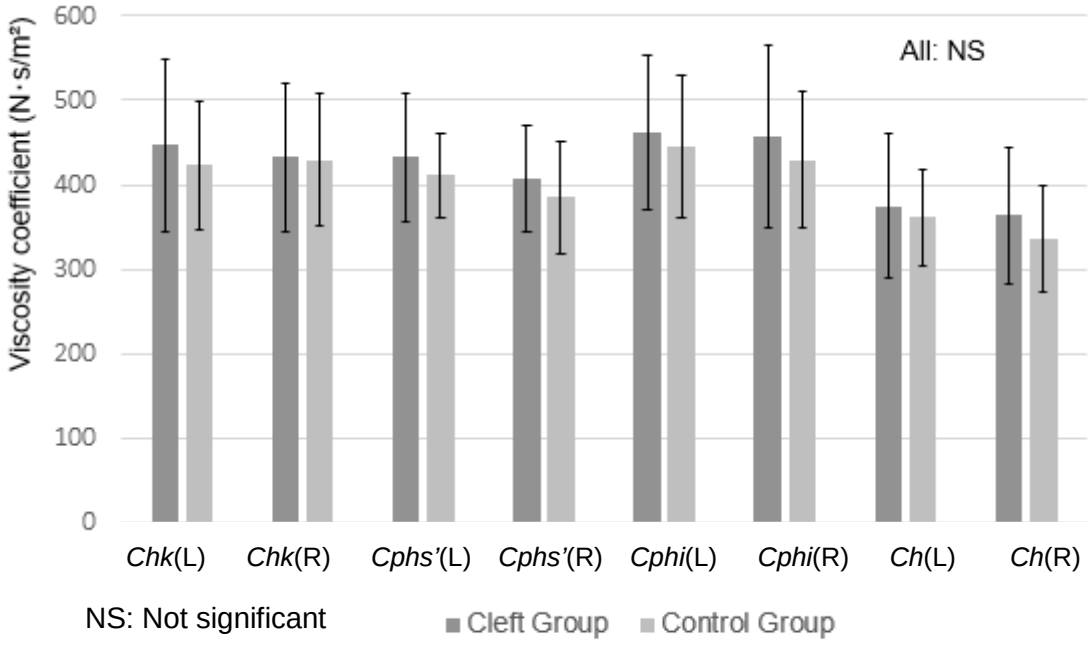
Viscosity coefficient (N·s/m²)
600
500
400
300
200
100
0
All: NS
Chk(L)
Chk(R)
Cphs'(L)
Cphs'(R)
Cphi(L)
Cphi(R)
Ch(L)
Ch(R)
NS: Not significant
Cleft Group
Control Group

Figure 10

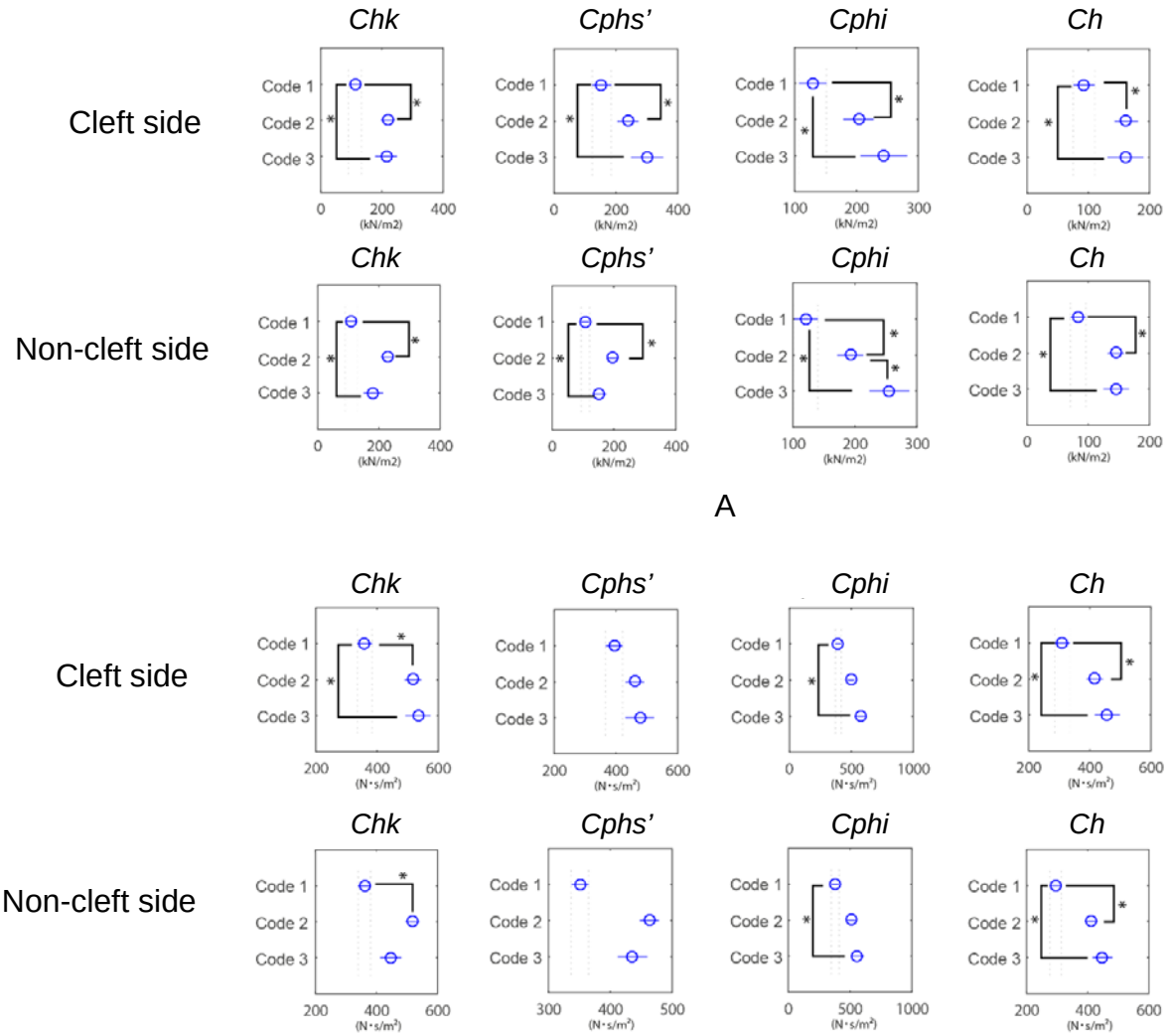

One-way ANOVA, Tukey post-hoc test: *P<0.05, Above MDC_{95} of each landmark

Figure 11

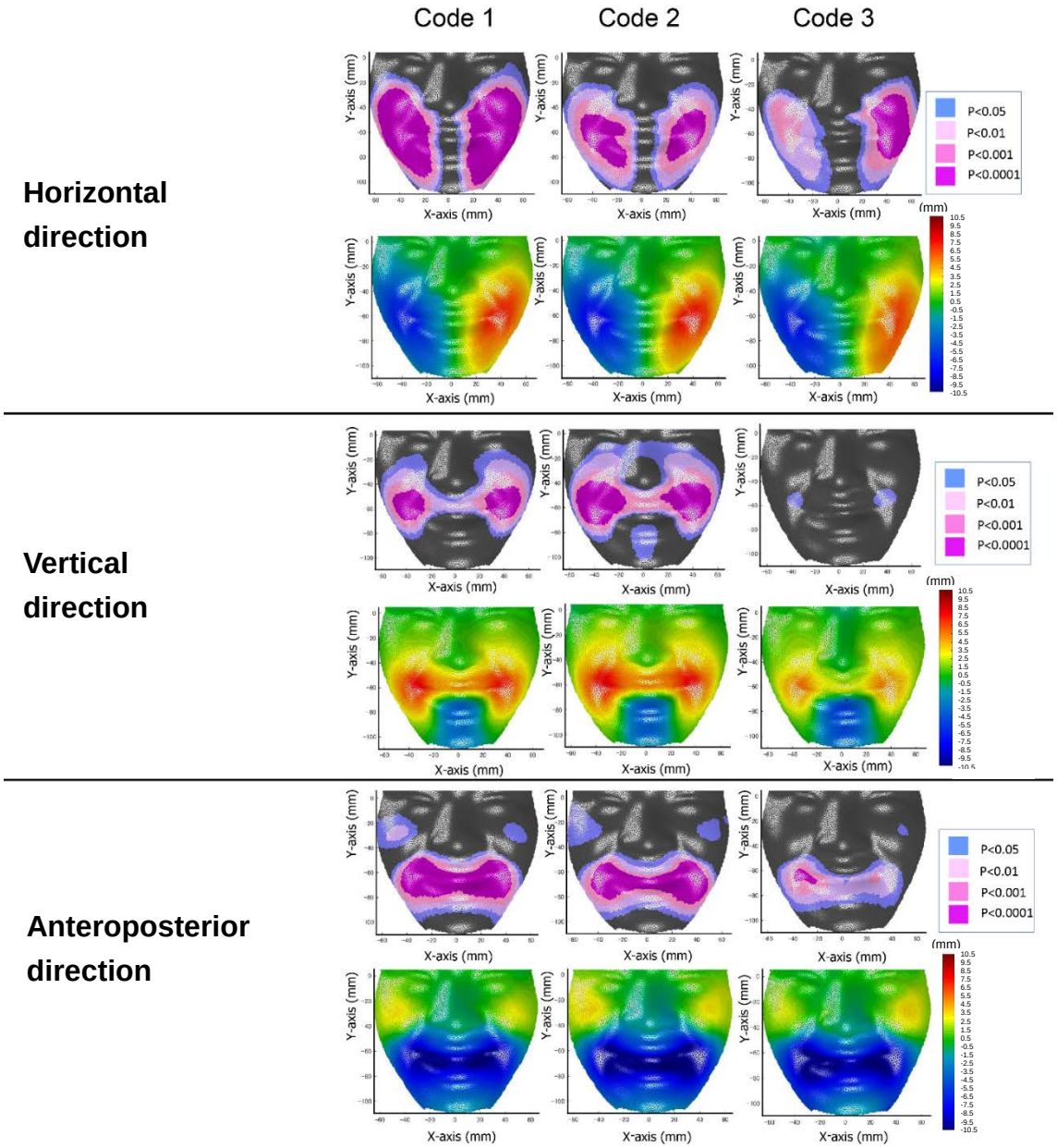
Code 1
Code 2
Code 3
Horizontal direction
Vertical direction
Anteroposterior direction
Y-axis (mm)
X-axis (mm)
P<0.05
P<0.01
P<0.001
P<0.0001
(mm)

Figure 12

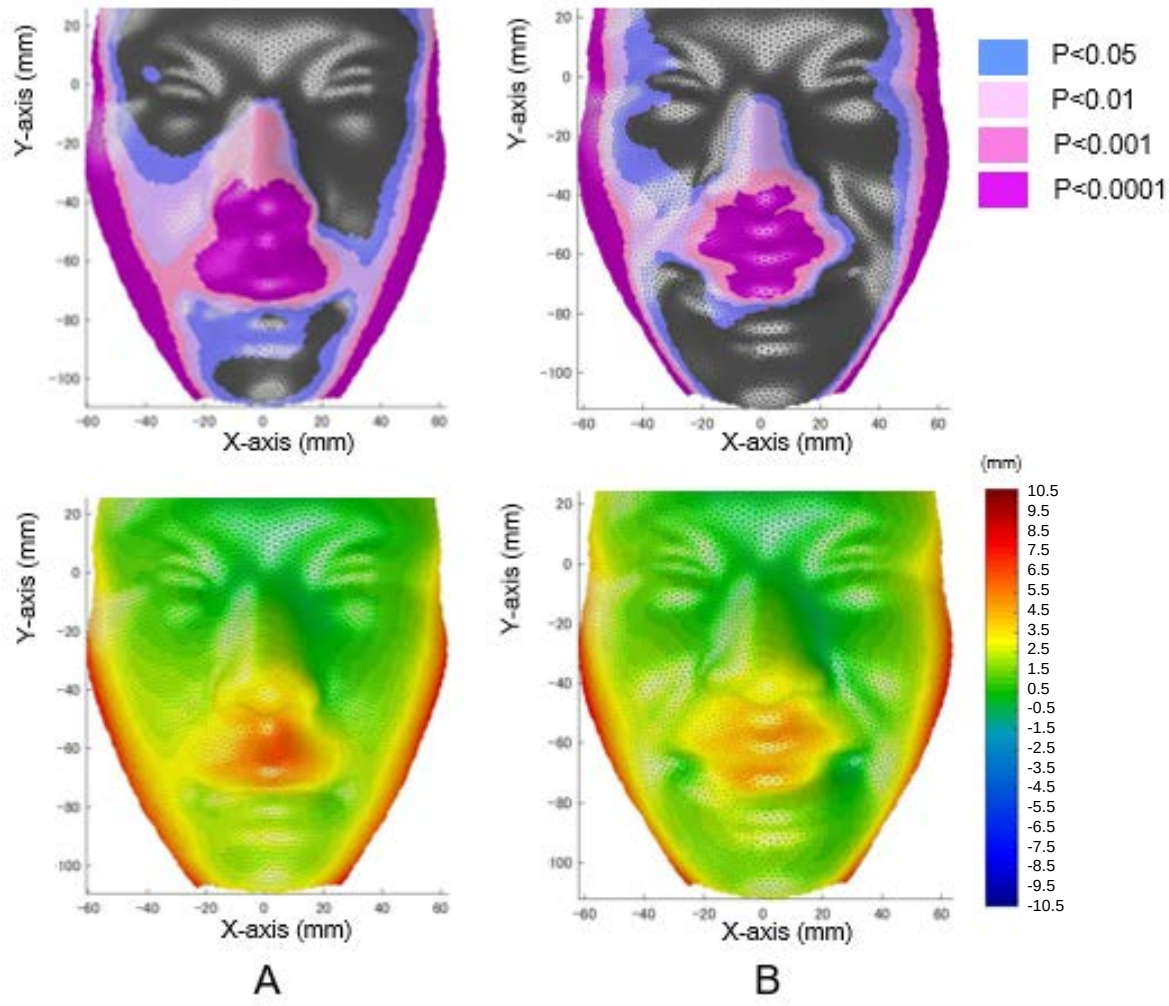

Supplementary Figure 1